Reprocessing VIIRS sensor data records from the early SNPP mission

Slawomir Blonski*[a] and Changyong Cao[b]
[a]Earth Resources Technology, Inc., College Park, MD, USA
[b]STAR/NESDIS, National Oceanic and Atmospheric Administration, College Park, MD, USA

ABSTRACT

The Visible-Infrared Imaging Radiometer Suite (VIIRS) instrument onboard the Suomi National Polar-orbiting Partnership (SNPP) satellite began acquiring Earth observations in November 2011. VIIRS data from all spectral bands became available three months after launch when all infrared-band detectors were cooled down to operational temperature. Before that, VIIRS sensor data record (SDR) products were successfully generated for the visible and near-infrared (VNIR) bands. Although VIIRS calibration has been significantly improved through the four years of the SNPP mission, SDR reprocessing for this early mission phase has yet to be performed. Despite a rapid decrease in the telescope throughput that occurred during the first few months on orbit, calibration coefficients for the VNIR bands were recently successfully generated using an automated procedure that is currently deployed in the operational SDR production system. The reanalyzed coefficients were derived from measurements collected during solar calibration events that occur on every SNPP orbit since the beginning of the mission. The new coefficients can be further used to reprocess the VIIRS SDR products. In this study, they are applied to reprocess VIIRS data acquired over pseudo-invariant calibration sites Libya 4 and Sudan 1 in Sahara between November 2011 and February 2012. Comparison of the reprocessed SDR products with the original ones demonstrates improvements in the VIIRS calibration provided by the reprocessing. Since SNPP is the first satellite in a series that will form the Joint Polar Satellite System (JPSS), calibration methods developed for the SNPP VIIRS will also apply to the future JPSS measurements.

Keywords: JPSS, SNPP, VIIRS, calibration, reprocessing

1. INTRODUCTION

The Visible-Infrared Imaging Radiometer Suite (VIIRS) instrument has been successfully operating onboard the Suomi National Polar-orbiting Partnership (SNPP) satellite since November 2011.[1] After launch, VIIRS was activated on November 8, 2011, and began acquiring Earth observations in the visible and near-infrared (VNIR) bands on November 21, 2011, when the nadir doors were opened on orbit #344. Shortly after the nadir doors opening, it was found that VIIRS responsivity in several spectral bands decreases with time much faster than expected, due to degradation of telescope mirrors.[2] Investigation of this anomaly has delayed opening of the cryoradiator door until January 18, 2012. The short-wave infrared (SWIR) and thermal emissive (TEB) bands that use cooled detectors began operating in nominal conditions on January 20, 2012. Initial optimization of the calibration parameters for all VIIRS bands was completed by February 6, 2012, and regular production of the VIIRS sensor data record (SDR) has began.

Before that day, VIIRS also acquired valid Earth observations, but calibration of the produced SDR was often non-optimal because of the telescope anomaly investigation. Nevertheless, the early VIIRS data are worthy reprocessing with optimized calibration, including the VNIR data since November 21, 2011, and the SWIR and TEB data since January 20, 2012. Calibration reanalysis for the reflective bands (VNIR and SWIR) has been recently completed based on processing parameters currently used in the operational VIIRS SDR production.[3] In this study, the new calibration coefficients were applied to reprocess VIIRS data acquired over the pseudo-invariant calibration sites Libya 4 and Sudan 1 in Sahara during the first 1500 orbits of the SNPP mission (until February 11, 2012). TEB and Day/Night Band (DNB) data were also reprocessed to demonstrate feasibility of applying the present operational approach to the early mission data.

*Slawomir.Blonski@noaa.gov, ph. 1-301-683-3603

Sensors, Systems, and Next-Generation Satellites XX, edited by Roland Meynart, Steven P. Neeck, Toshiyoshi Kimura, Haruhisa Shimoda, Proc. of SPIE Vol. 10000, 1000015 · © 2016 SPIE
CCC code: 0277-786X/16/$18 · doi: 10.1117/12.2241423

2. METHODS AND MATERIALS

Details of the reprocessing methodology have been described previously.[3] One should note that the calibration coefficients from the reanalysis are optimized for the VNIR and SWIR bands only. To improve DNB calibration, additional relative spectral response (RSR) tables were created to account for DNB RSR changes due to the telescope degradation. Other DNB processing parameters, as well as those used for TEB, were the same as in the present operational SDR production.

Raw data record (RDR) inputs and original SDR products were obtained from the Comprehensive Large Array-data Stewardship System (CLASS) archive maintained by the National Oceanic and Atmospheric Administration (NOAA) (http://www.class.noaa.gov/). Only five strictly cloud-free datasets with near-nadir observations of two calibration sites, Libya 4 and Sudan 1, were selected for the reprocessing (Table 1). While the day-time, near-nadir observations are acquired every 16 days for each site, many of the datasets from the early SNPP mission include clouds. Some of the observations were also not acquired because of the ongoing telescope anomaly investigation.

Table 1. List of the reprocessed VIIRS SDR granules.

Date/Time (UTC)	Orbit #	Site
2011-12-01 11:30-11:31	484	Libya 4
2011-12-07 11:16-11:17	569	Sudan 1
2012-01-08 11:15-11:16	1023	Sudan 1
2012-01-18 11:29-11:30	1165	Libya 4
2012-01-24 11:15-11:16	1250	Sudan 1

3. VNIR REPROCESSING

3.1 Solar diffuser degradation

Since VIIRS on-orbit, solar calibration is based on measurements of light reflected from the onboard solar diffuser, knowledge of the diffuser reflectance is fundamental for calibration accuracy. Changes in the solar diffuser's reflectance with time are measured by a separate, onboard instrument: the SDSM (Solar Diffuser Stability Monitor). SDSM measurements are used to derive for each band an H factor: a ratio of the current diffuser reflectance to its value at the beginning of the mission. While the H factors are directly used to scale the calibration coefficients for the VNIR bands, degradation of the solar diffuser reflectance is considered negligible for the SWIR bands during the early months of the SNPP mission.

During the early operations after launch, SDSM measurements were conducted once per orbit, with the exceptions of several gaps in the VIIRS data due to the telescope anomaly investigation and the once-per-day frequency for five days after the cryoradiator door opening. The H factors calculated from these measurements are shown in Figure 1. Operational calculations of the H factors include smoothing and extrapolation with the Robust Holt-Winters (RHW) filter.[4] Because the RHW filter introduces transient effects for few days after initialization, H factors calculated both with and without the filtering are shown in Figure 1. The RHW transient effects clearly diminish before the earth observations have began, as indicated in the figure. However, smaller transient effects can be seen after each longer data gap. Nevertheless, the RHW filter has successfully extrapolated the H factors from the once-per-day SDSM measurements near orbit #1200.

Rate of the diffuser degradation is the fastest at the shortest wavelengths for band M1 (412 nm), and then decreases with the band center wavelength from M2 (445 nm), through M3 (488 nm), M4 (555 nm), M5 (672 nm), M6 (746 nm), to M7

(865 nm). This wavelength dependence of the degradation rate can be explained by Rayleigh scattering that is induced by surface roughness, since the VIIRS solar diffuser is made from a porous material with a high surface area.[5]

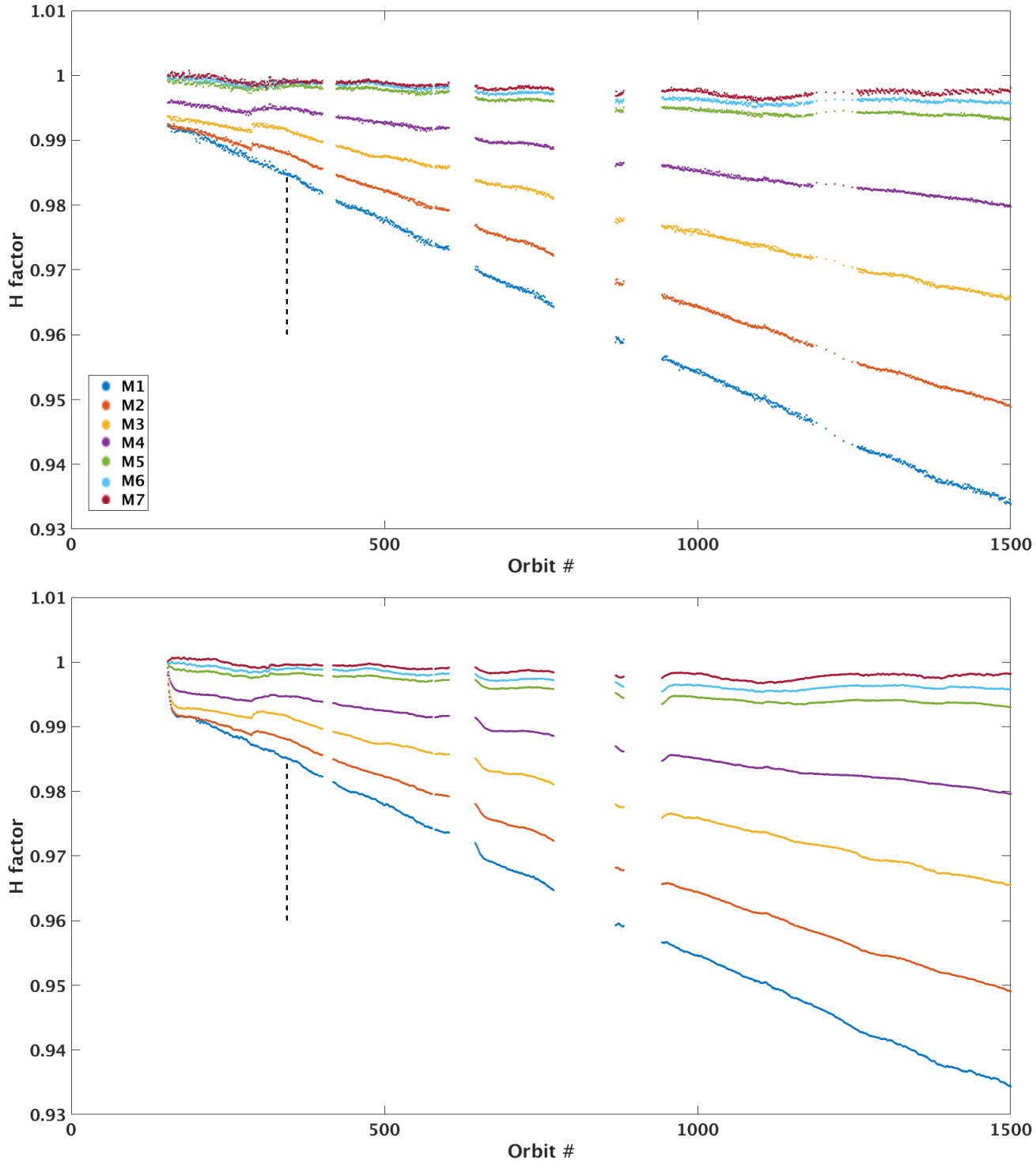

Figure 1. Degradation of the SNPP VIIRS solar diffuser reflectance (the H factor) for the VNIR bands M1–M7 as measured by the SDSM during the first 1500 orbits and analyzed with (bottom) and without (top) the RHW filtering. The vertical dashed lines indicate orbit #344 when the nadir doors were opened.

Without the RHW filtering, the initial H factor trends for all bands seem to be converging, as should be expected, to the value of one at the zero orbit (i.e., at launch). With some variability clearly present in the H factor time series, the convergence may not be exact, and this indicates uncertainties in monitoring of the solar diffuser degradation. A small increase in the degradation rate may be seen after the nadir doors opening, but it is definitely not as large as reported in other studies.[6,7] The much larger acceleration of the degradation is implausible. Illumination of the solar diffuser is measured by VIIRS for a short time during each scan. Despite scarcity of the measurements, the data are quite smooth, as shown in Figure 2, and one can hardly suspect any unexpected illumination increases between the measurements. Figure 2 shows the diffuser illumination during the last orbit before the nadir doors opening (#343) and the first orbit after the doors were opened (#345). Before the doors opening, the diffuser is only directly illuminated by the sun, through an attenuation screen. After the doors are opened, the diffuser is additionally illuminated by the sunlight reflected from the earth surface and atmosphere, as can be seen in Figure 2. From the comparison of the before and after data, the total earthshine contribution on one orbit is estimated to be only about 30% of the direct solar illumination. This contradicts the claim by Sun and Wang that the earthshine contribution is twice as large as the direct solar one.[6] While the presented analysis is done at the wavelength of 412 nm, similar proportions can be expected in the ultraviolet that is responsible for the diffuser degradation. Temporal evolution of the derived H factors is sensitive to vignetting and bidirectional reflectance parameters used in the calculations, and the observed differences in the calculated H factors again indicate uncertainties in the solar diffuser reflectance monitoring.

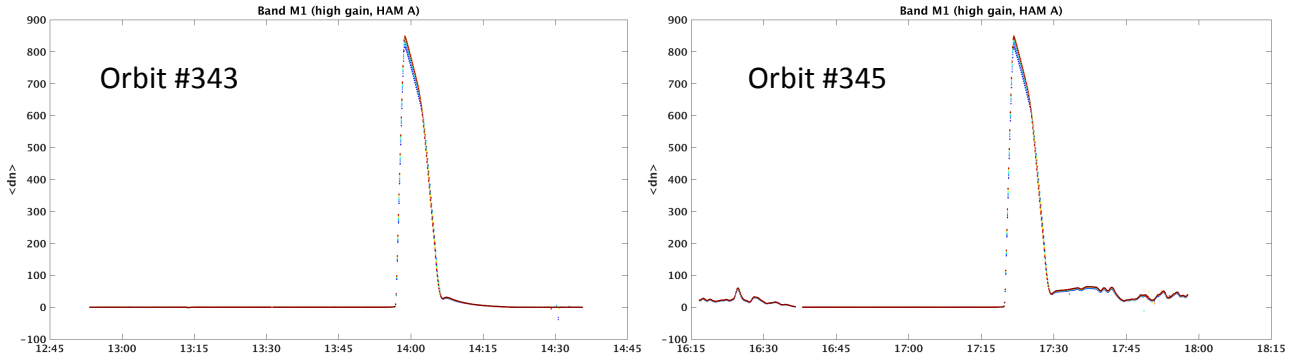

Figure 2. VIIRS channel M1 solar diffuser measurements acquired during the last orbit before the nadir doors opening (left) and the first orbit after the doors were opened (right) on November 21, 2011. Space view measurements have been subtracted from the solar diffuser data. Measurements acquired with high gain and with one side of the half-angle mirror (HAM) are shown. Data for each detector are shown in a different color.

3.2 Calibration coefficients

VIIRS VNIR and SWIR radiometric calibration coefficients are products of coefficients derived from prelaunch tests and scaling factors F derived from on-orbit solar calibration measurements. The F factors provide scaling between the prelaunch testing and on orbit performance, and they characterize most (but not all) of the calibration coefficient changes occurring on orbit.[3] During the calibration reanalysis, the F factors were calculated both with and without the RHW filtering, to assess transient effects of applying the RHW filter. For every reflective band, the F factors are calculated separately for each detector, HAM side, and gain state (for dual-gain bands). Figure 3 shows the F factors calculated in the calibration reanalysis for band M1. Temporal evolution of the M1 F factors is quite consistent among detectors, HAM sides, and gain states, and only small radiometric response degradation (F factor increase) with time can be observed. Comparison of the F factors calculated with and without the RHW filtering shows that transient effects created by the filter diminish before the commencement of the earth observations and thus do not affect calibration of the VIIRS SDR products. Similar F factor changes can be seen for the other bands that are only marginally affected by the telescope degradation: M2, M3, and M4.

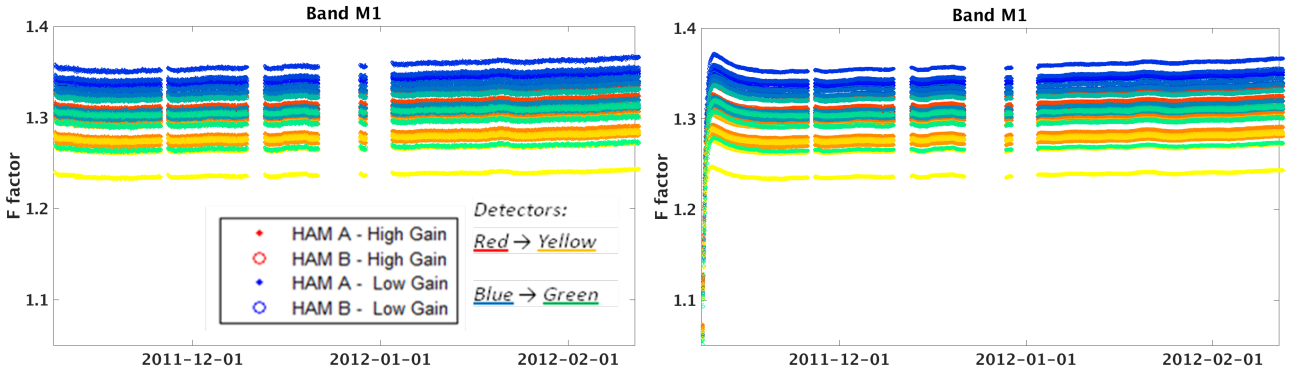

Figure 3. F factors calculated for the VIIRS band M1 without (left) and with (right) the RHW filtering for the first 1500 orbits of the SNPP satellite. The HAM sides are indicated by different symbols (dots and circles), while the F factors are shown for each detector with a different color from the red-yellow (for high/single gain) and blue-green (for low gain) palettes.

VIIRS telescope degradation has the largest effect on band M7.[8] F factors calculated for band M7 are shown in Figure 4. An onset of the telescope degradation when the nadir doors were opened on November 21, 2011, can be clearly identified on the graphs. The degradation has slowed down significantly during several periods when VIIRS earth observations were suspended, but otherwise it progressed rapidly during the early weeks of the SNPP mission: the M7 F factors increased about 20% by February 11, 2012. Transient RHW filter effects can be seen shortly after initialization of the solar calibration measurements, but they diminish before the earth observations began. The transient effects can be also seen after each, multi-orbit gap in the measurements, although they are much smaller than the overall F factor changes from the telescope degradation. Comparison of the F factors derived with and without the RHW filtering shows that these transient artifacts can be removed in the calibration reanalysis that is based not on extrapolation, but rather on interpolation of the solar measurements. Similar F factor time series are produced for the other VNIR bands affected by the telescope degradation, but with the degradation rate increasing from M5 through M6 to M7.

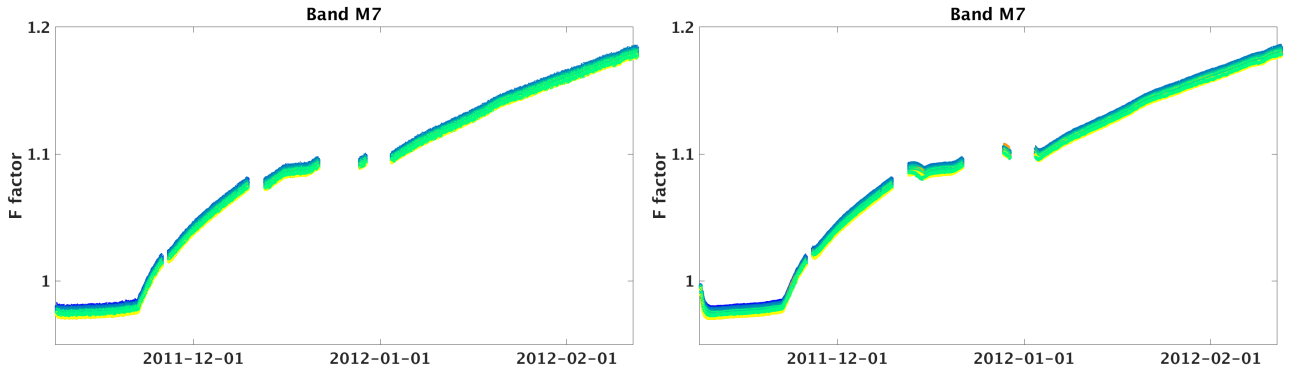

Figure 4. F factors calculated for the VIIRS band M7 without (left) and with (right) the RHW filtering for the first 1500 orbits of the SNPP satellite. The HAM sides are indicated by different symbols (dots and circles), while the F factors are shown for each detector with a different color from the red-yellow (for high/single gain) and blue-green (for low gain) palettes.

3.3 Calibration site data reprocessing

An example of the original and reprocessed VIIRS SDR data acquired on December 1, 2011, is shown in Figure 5. The two data granules that are shown in each image provide the first near-nadir VIIRS measurements from the Saharan calibration site Libya 4. Reprocessing has removed the data gaps that existed in the original products and has reduced the

faint striping that can be seen over uniform desert areas. Figure 5 confirms that overall quality of the VIIRS data from the early SNPP mission is good and the VNIR data are suitable for reprocessing.

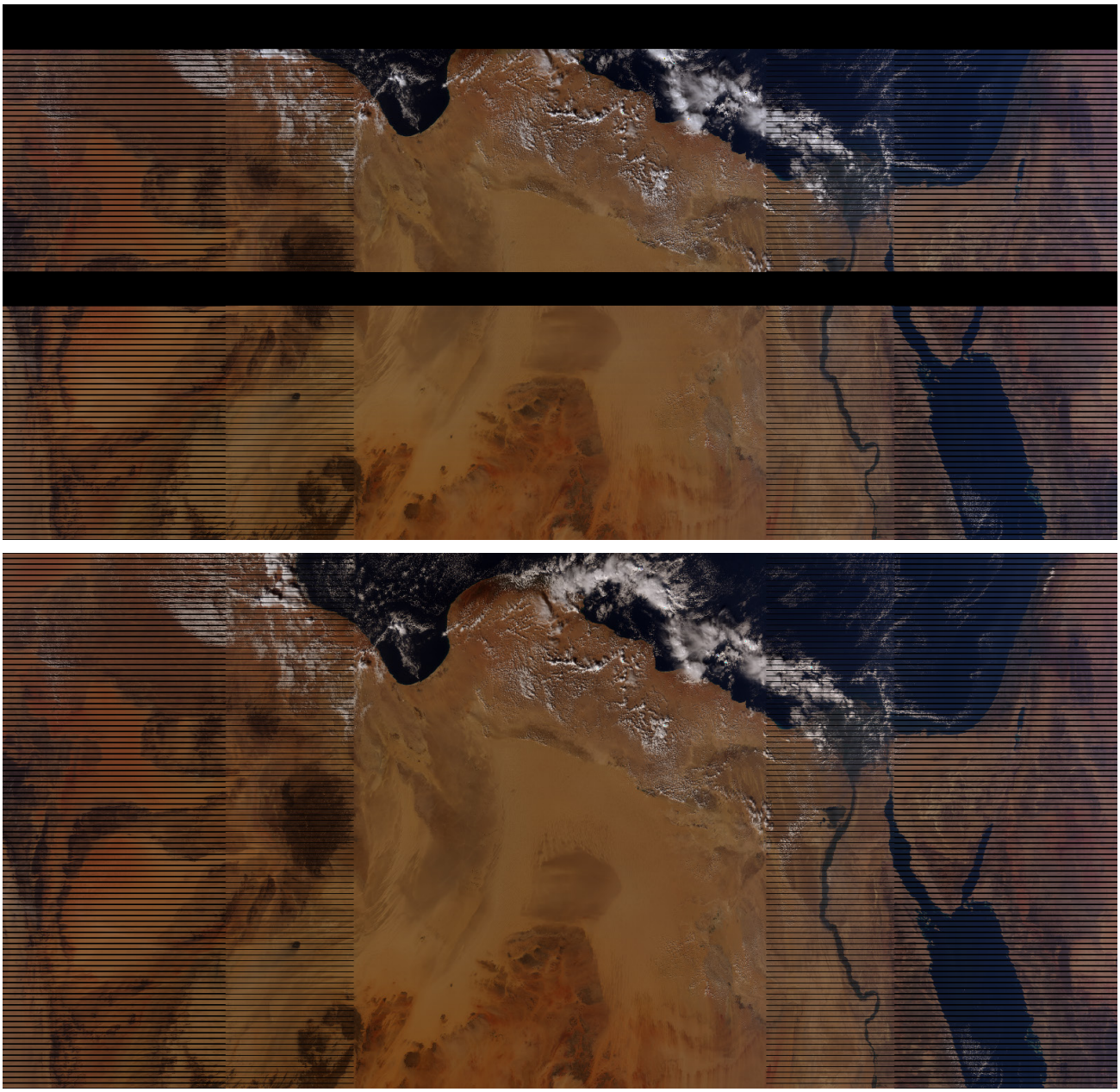

Figure 5. Full-swath images of the Saharan Desert created from two granules of the original (top) and reprocessed (bottom) VIIRS SDR data acquired on December 1, 2011. Top-of-atmosphere (TOA) reflectance in bands M5, M4, M2 is shown as the RGB colors (with square root stretching applied). Data gaps in the original products are visible as the wide black stripes. "Bow-tie" deletion creates the 2- and 4-pixel dark stripes towards the ends of each scan, but full spatial coverage is provided by overlap existing between scans in those areas.

A subset of the data from Figure 5 that includes the Libya 4 site is shown in Figure 6, with a geographic projection applied to the images. Analogous images for the Sudan 1 site are also shown in this figure. In addition to the striping

reduction, the figure also illustrates a 1-2 km geolocation change created by parameter improvements introduced in the operational SDR production between the original processing and the reprocessing.[9] While the geolocation change results in slightly different pixels being selected for comparisons between the original and reprocessed data from the calibration sites, uniformity of the surrounding desert areas makes this spatial shift negligible. To ensure full coverage of the Libya 4 calibration site, two granules were analyzed together in that case.

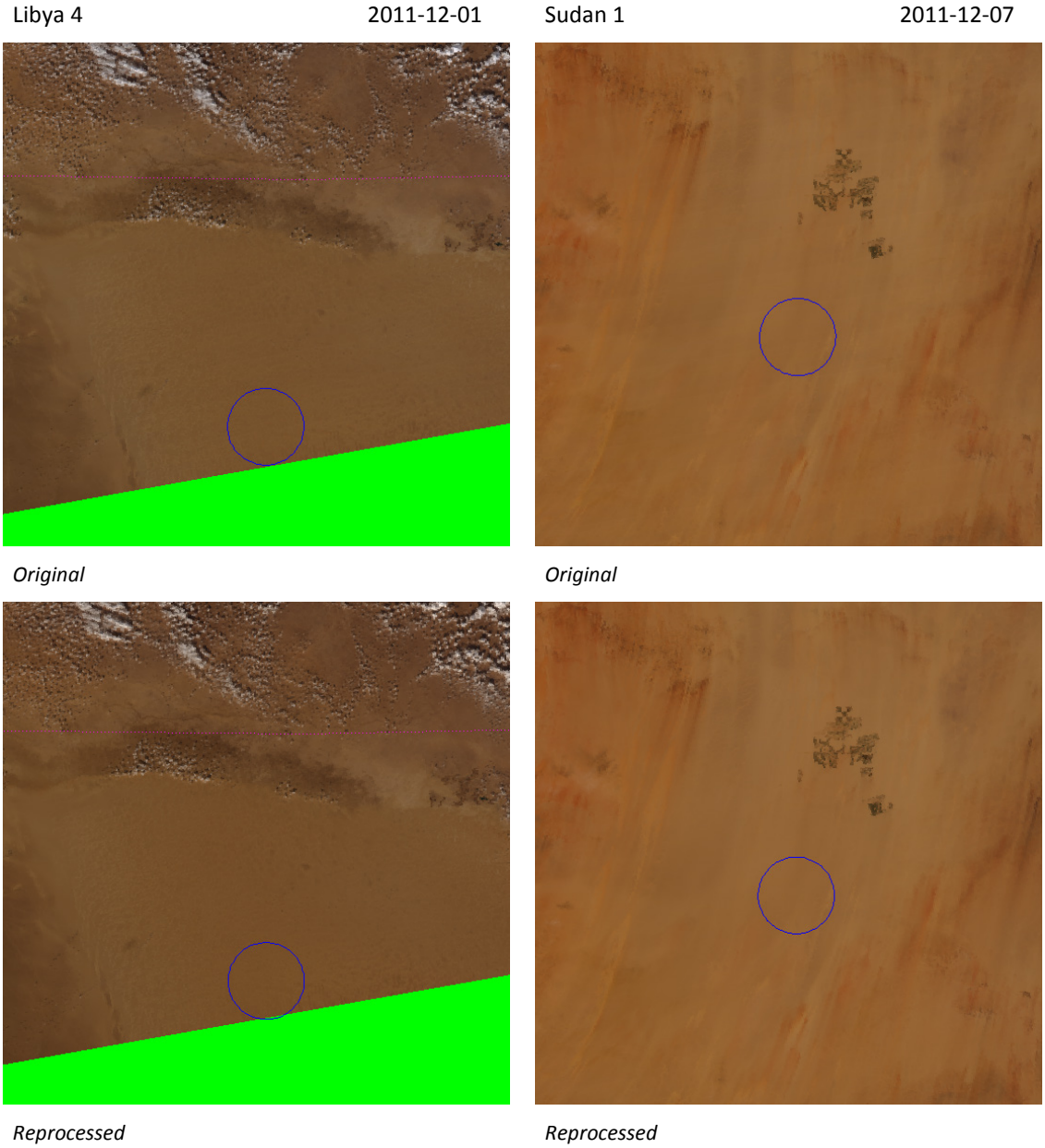

Figure 6. Reprojected images of the Saharan calibration sites Libya 4 (left) and Sudan 1 (right) created from the original (top) and reprocessed (bottom) VIIRS SDR data. Top-of-atmosphere (TOA) reflectance in bands M5, M4, M2 is shown as the RGB colors (with square root stretching applied). Blue circles indicate 50-km diameter areas selected for the comparisons. Data from only one granule are shown for the Libya 4 site to illustrate the geolocation difference.

While only two datasets are shown in Figure 6, all five datasets from the Libya 4 and Sudan 1 calibration sites were analyzed, and the results for the original and reprocessed data are shown on graphs in Figure 7 for each of the bands M1

to M5 and M7 (desert sites measurements for M6 exceed its dynamic range). Although variability of the measured reflectance exists for each site and between the two sites, reprocessing with the optimized calibration clearly improves stability and consistency of the measurements for bands M1, M2, and M7. For bands M3 and M4, improvements in stability are small, but consistent shifts in reflectance measurements can be seen. Validity of these shifts can be established by comparisons with reprocessed VIIRS SDR data from a longer time period. Somewhat surprisingly, the original and reprocessed M5 reflectance values are similar, and any improvement can be hardly seen for the M5 data from the early SNPP mission.

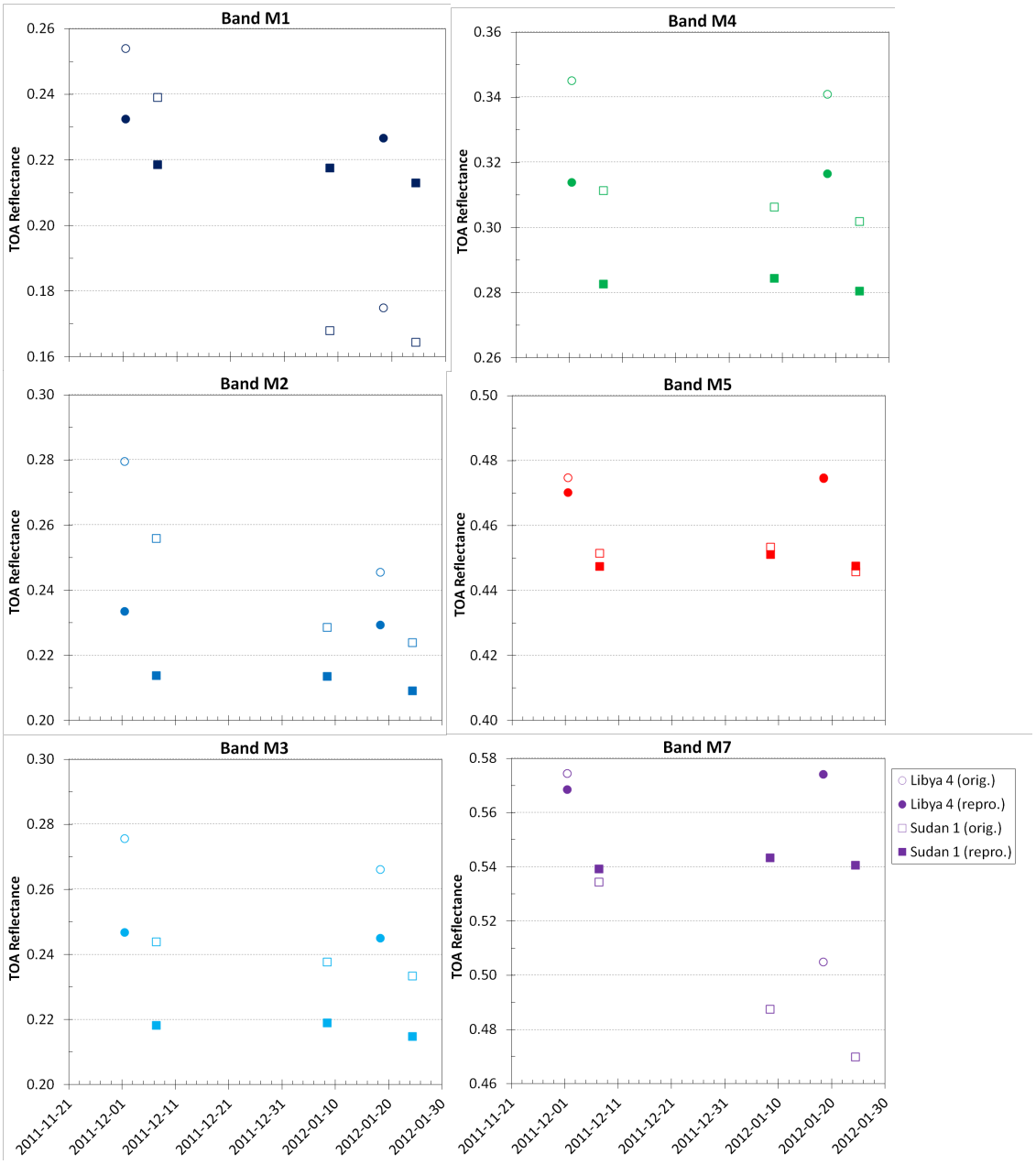

Figure 7. Comparisons of the original (open symbols) and reprocessed (filled symbols) VIIRS SDR TOA reflectance measurements acquired over the Saharan calibration sites Libya 4 (circles) and Sudan 1 (squares) during the early months of the SNPP mission.

4. SWIR REPROCESSING

4.1 Calibration coefficients

When the cryoradiator door was opened on January 18, 2012, the cool-down of the SWIR detectors has begun. The detectors reached an operational temperature by midday on January 20, 2012 (Figure 8).

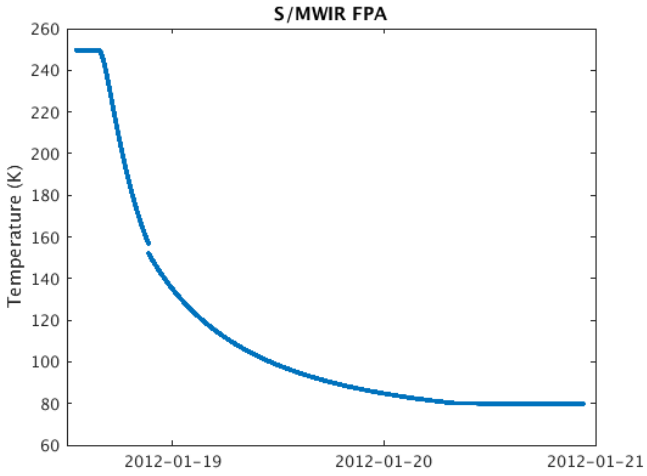

Figure 8. Temperature of the SWIR detector array measured during the initial cool-down after the SNPP VIIRS cryoradiator door opening.

When the operational temperature was reached, noise in the cooled detectors for the SWIR bands, as well as for DNB and TEB, has diminished and detector gains have stabilized. However, the gains for the SWIR bands did not become completely stable because the SWIR bands have also been affected by the progressing SNPP VIIRS telescope throughput degradation. Figure 9 shows the F factors derived from the solar calibration measurements for band M10 (1,610 nm). After the quick initial adjustment following the cool-down, the M10 F factors began a steady increase with time due to the telescope degradation. Small transient effects can be seen at the beginning when the RHW filter is applied, but they diminish within one week. Similar F factor time series are produced for the other SWIR bands, but with the telescope throughput degradation rate decreasing with band center wavelength from M8 (1,240 nm) through M9 (1,378 nm) and M10 to M11 (2,250 nm).

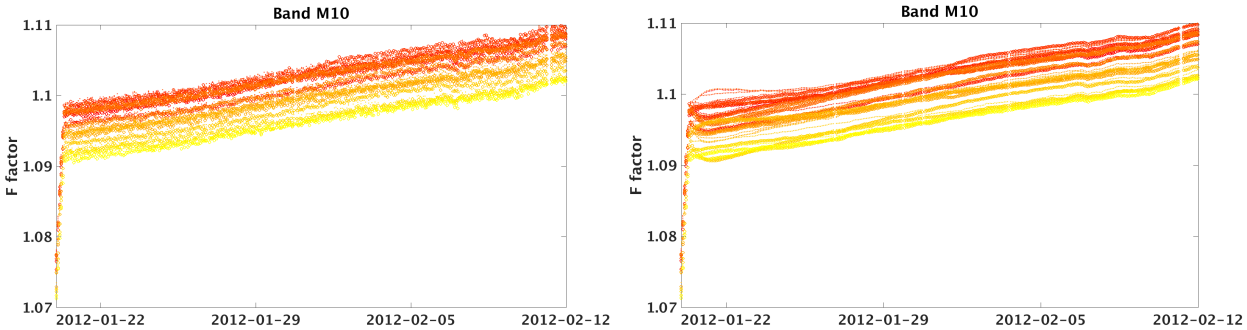

Figure 9. F factors calculated for the VIIRS band M10 without (left) and with (right) the RHW filtering for the time period between the detector cool-down and the 1500th orbit of the SNPP satellite. The HAM sides are indicated by different symbols (dots and circles), while the F factors are shown for each detector with a different color from the red-yellow palette (for single gain).

4.2 Calibration site data reprocessing

An example of reprocessed VIIRS SDR data from the SWIR bands is shown in Figure 10. With the radiometric stretching applied, the original and reprocessed SWIR images look similar, and both display good data quality. However, reprocessing with the optimized calibration coefficients changes the reflectance measurements by at least several percent. Scatter plots in Figure 11 show high correlation between the original and reprocessed SWIR products, but the measurements that are corrected by taking into account the telescope throughput degradation are clearly different.

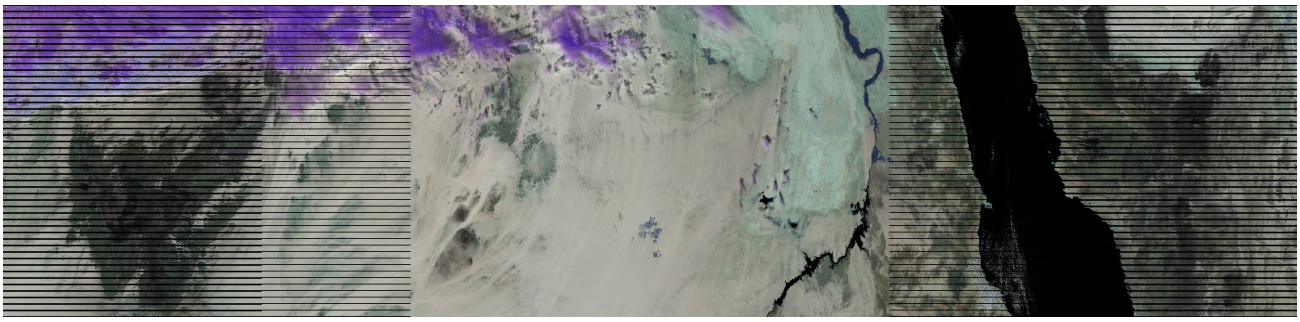

Figure 10. A full-swath image of the Saharan Desert created from the reprocessed VIIRS SDR data acquired on January 24, 2012. Top-of-atmosphere (TOA) reflectance in bands M11, M10, M8 is shown as the RGB colors (with linear stretching applied). "Bow-tie" deletion creates the 2- and 4-pixel dark stripes towards the ends of each scan, but full spatial coverage is provided by overlap existing between scans in those areas.

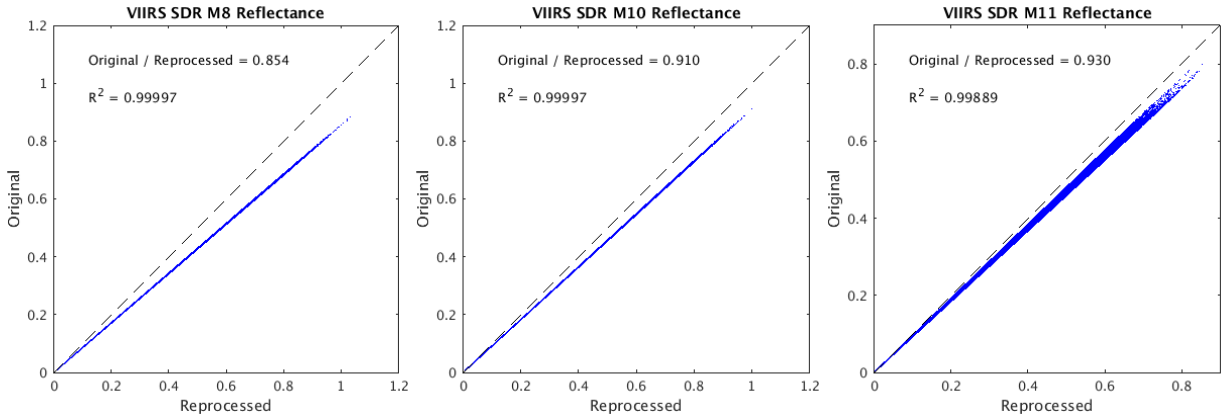

Figure 11. Comparisons of the original and reprocessed TOA reflectance measurements in the SWIR bands M8 (left), M10 (center), and M11 (right) for the granule shown in Figure 10.

5. TEB REPROCESSING

Figure 12 shows the original and reprocessed VIIRS SDR brightness temperature products created for band M16 (12.013 μm) from data acquired on January 24, 2012. Cold clouds, hot desert, and warm sea and inland waters can be identified in the images. While the images in Figure 12 are similar, Figure 13 shows that the differences between the original and reprocessed M16 products are around 0.03-0.04% (~0.1 K). Differences for the other single-gain thermal bands, M12 (3.700 μm), M14 (8.550 μm), and M15 (10.763 μm) are comparable, but the differences from the reprocessing are sometimes larger for the dual-gain band M13 (4.050 μm) because of a code correction implemented for this band (Figure 13).

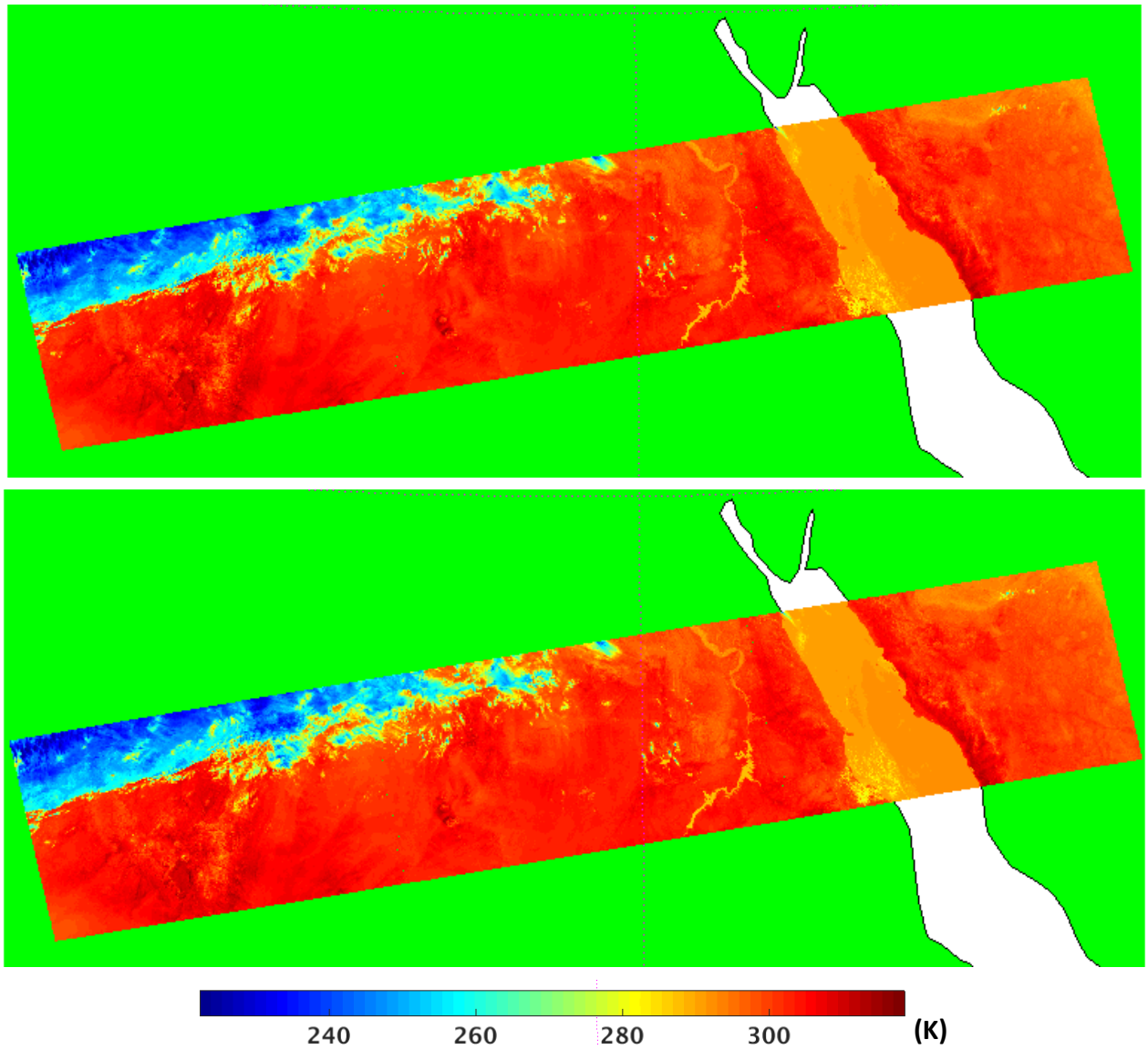

Figure 12. Reprojected full-swath images created from the original (bottom) and reprocessed (top) band M16 brightness temperature products using SNPP VIIRS data acquired on January 24, 2012.

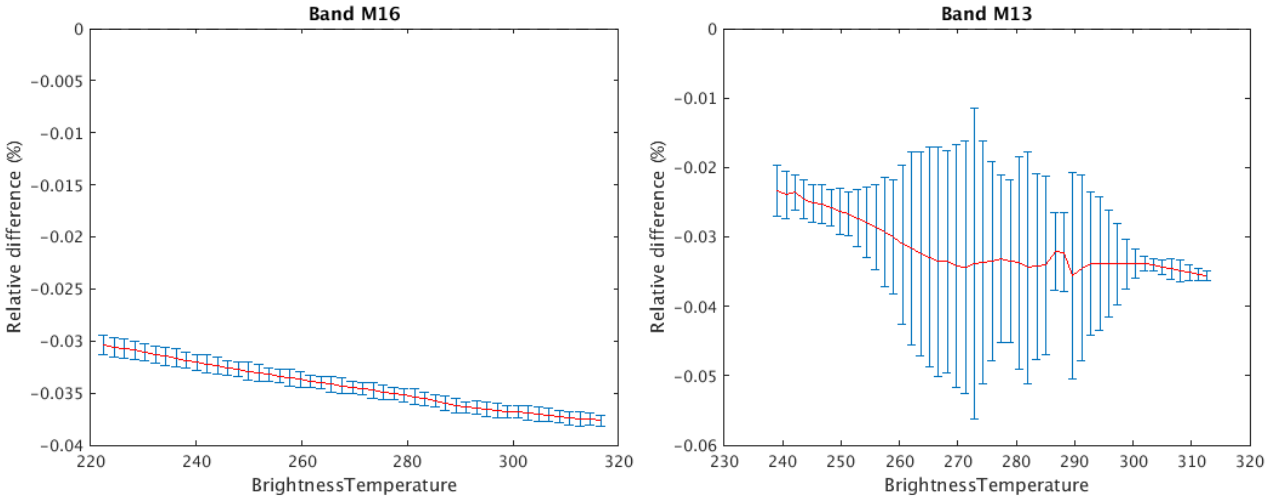

Figure 13. Relative differences (red lines) between the original and reprocessed brightness temperature products (in K) for bands M16 (left) and M13 (right). All data from the granule shown in Figure 12 are included in the comparison. Error bars (blue) show standard deviation of the differences.

6. DNB REPROCESSING

6.1 Calibration coefficients

DNB radiometric calibration coefficients for the Low-Gain Stage (LGS) are called the LGS gains. Only the LGS gains are directly determined from the solar diffuser measurements. Calibration coefficients for the Mid- and High-Gain Stages are calculated from ratios to the LGS gains. To keep pixel size near constant across the full swath, DNB onboard processing includes 32 different aggregation modes. Since each aggregation mode is calibrated separately, DNB solar calibration cannot be completed during one orbit, as is the case for the other reflective bands, and the RHW filter had to be always applied in the LGS gain reanalysis. Results of the DNB LGS gain calculations for two of the aggregation modes are shown in Figure 14. Transient effects from the RHW filter can be seen, but they do not obscure the onset of effects from the telescope degradation. For DNB, not only the radiometric response, but also the spectral response is affected by the telescope throughput changes. The LGS gains have increased by approximately 10% during the first 1500 orbits of the SNPP mission. Another transition period can be seen after the cool-down of the DNB detector arrays has started on January 18, 2012, and the gains adjusted to the new operating temperature.

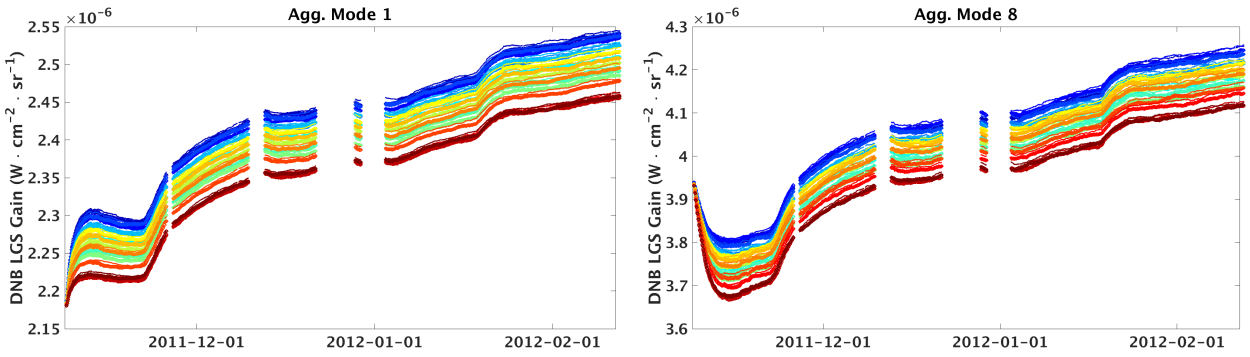

Figure 14. DNB LGS gains calculated for the aggregation modes 1 (left) and 8 (right) for the first 1500 orbits of the SNPP satellite. The HAM sides are indicated by different symbols (dots and circles) while data for each of the 16 detectors are shown in a different color.

6.2 Calibration site data reprocessing

Examples of DNB images produced in the reprocessing are shown in Figure 15. Despite being acquired before the cool-down of the DNB detectors, the images display good quality, although some striping can be seen near the swath edges. One should note that the presented reprocessing shall be applied only to DNB data acquired during daytime. For nighttime scenes, additional improvements to DNB processing parameters should be implemented, including dark offsets, gain ratios, and straylight correction, but such changes are beyond scope of this study.

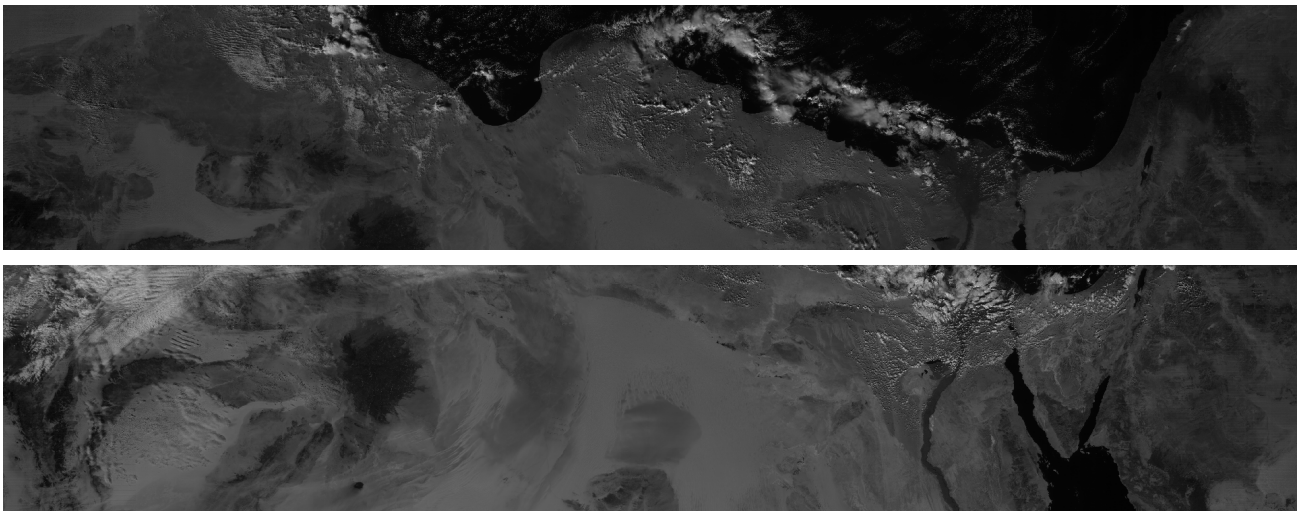

Figure 15. Full-swath images created from DNB data acquired on December 1, 2011 (top) and January 18, 2012 (bottom).

7. DISCUSSION AND CONCLUSIONS

This study has demonstrated that VIIRS SDR from the early months of the SNPP mission can be successfully reprocessed using optimized calibration coefficients currently applied in the operational SDR production. Suitable for reprocessing are VNIR and daytime DNB data acquired since November 21, 2011, as well as SWIR and TEB data acquired since January 20, 2012. Over Saharan pseudo-invariant calibration sites, the reprocessed SDR datasets provide measurements that are more consistent and stable than those from the original SDR, despite the telescope throughput degradation that was quickly progressing during that time.

While this study shows benefits of applying the current operational VIIRS SDR processing to data from the beginning of the SNPP mission, further improvements to the calibration parameters are still possible. The operational system generates VIIRS SDR products in near real time with latency currently limited to no more than few hours. For the VNIR and SWIR bands, the applied calibration coefficients cannot be based solely on interpolation between existing solar calibration measurements, and an extrapolation of the coefficients into the future is always required. Reprocessing that uses this approach provides the SDR products that are most consistent with the latest operational output, but it may be less accurate than reprocessing that is based only on the interpolation.

Radiometric calibration of the VIIRS reflective bands depends on monitoring reflectance of the onboard solar diffuser by the SDSM. SDSM measures diffuser's reflectance from a viewing direction that is different than the direction used by the VIIRS telescope during solar calibration measurements. Calibration coefficients are calculated from the solar measurements with an assumption that the diffuser degradation is isotropic, i.e., that H factors in both directions are the same. Deviations from this assumption can be detected and corrected using lunar calibration.[10] However, VIIRS lunar calibration measurements in January and February 2012 were conducted with a different lunar phase angle than during the later moon observations, and uncertainty of these early lunar data may be larger than the later ones, which started in April 2012. Therefore, the early lunar calibration data may not be suitable for correcting radiometric calibration for the VIIRS data from the beginning of the SNPP mission.

SNPP is the first satellite in a series that will form the Joint Polar Satellite System (JPSS) deployed by the National Oceanic and Atmospheric Administration (NOAA) and the National Aeronautics and Space Administration (NASA) of the United States. Calibration methods developed for the SNPP VIIRS have improved the current operational data products and will also apply to the future JPSS measurements. Accurate calibration ensures continuity of the satellite measurements for operational weather forecasting and climate change studies.

ACKNOWLEDGEMENTS

This work was partially funded by the JPSS program office and by the NOAA contract DG133E-12-CQ-0020. The manuscript contents are solely the opinions of the authors and do not constitute a statement of policy, decision, or position on behalf of NOAA or the U.S. government.

REFERENCES

[1] Cao, C. *et al*., "Suomi NPP VIIRS sensor data record verification, validation, and long-term performance monitoring," J. Geophys. Res. Atmos. 118, 11664–11678 (2013). DOI 10.1002/2013JD020418 and 10.1002/jgrd.51282.

[2] De Luccia, F., *et al*., "Discovery and characterization of on-orbit degradation of the Visible Infrared Imaging Radiometer Suite (VIIRS) Rotating Telescope Assembly (RTA)," Proc. SPIE 8510, 85101A (2012). DOI 10.1117/12.930544.

[3] Blonski, S., and Cao, C., "Suomi NPP VIIRS Reflective Solar Bands Operational Calibration Reprocessing," Remote Sens. 7(12), 16131-16149 (2015). DOI 10.3390/rs71215823.

[4] Rausch, K. *et al*., "Automated calibration of the Suomi National Polar-Orbiting Partnership (S-NPP) Visible Infrared Imaging Radiometer Suite (VIIRS) reflective solar bands," J. Geophys. Res. Atmos. 118, 13434–13442 (2013). DOI 10.1002/2013JD020479.

[5] Shao, X., Cao, C. and Liu, T.-C., "Spectral dependent degradation of the solar diffuser on Suomi-NPP VIIRS due to surface roughness-induced Rayleigh scattering," Remote Sens. 8(3), 254 (2016). DOI 10.3390/rs8030254.

[6] Sun, J., and Wang, M., "Visible Infrared Imaging Radiometer Suite solar diffuser calibration and its challenges using a solar diffuser stability monitor," Appl. Optics 53(36), 8571-8584 (2014). DOI 10.1364/AO.53.008571.

[7] Lei, N., and Xiong, X., "Estimation of the accuracy of the SNPP VIIRS SD BRDF degradation factor determined by the Solar Diffuser Stability Monitor," Proc. SPIE 9607, 96071V, (2015). DOI 10.1117/12.2186636.

[8] Blonski, S., and Cao, C., "Monitoring and predicting rate of VIIRS sensitivity degradation from telescope contamination by tungsten oxide," Proc. SPIE 8739, 87390D (2013). DOI 10.1117/12.2016008.

[9] Wolfe, R. E., *et al*., "Suomi NPP VIIRS prelaunch and on-orbit geometric calibration and characterization," J. Geophys. Res. Atmos., 118, 11508–11521 (2013). DOI 10.1002/jgrd.50873.

[10] Xiong, X. *et al*., "Lunar calibration and performance for S-NPP VIIRS reflective solar bands," IEEE Trans. Geosci. Remote Sens. 54(2), 1052-1061 (2016). DOI 10.1109/TGRS.2015.2473665.